TECHNICAL PAPER

Suppression of chaotic vibrations in suspension system of vehicle dynamics using chattering-free optimal sliding mode control

S. Mahdi Abtahi[1]

Abstract

In this wok, chaos analysis along with chaos control is studied in vertical model of the vehicle system. The chaotic behavior has been demonstrated in the suspension system under the specific initial conditions, values of parameters, and profile of road roughness. In order to analyze chaos in the dynamical model, the power spectrum density and Lyapunov exponent methods are used. Moreover, the phase portrait and Poincare' sections of the simulations verify numerically chaos in uncontrolled system. For the purpose of chaos control, a novel optimal sliding mode control strategy is designed for stabilization of the system's behavior via the semi-active suspension using MR fluid damper. As results, the optimal sliding mode control eliminates the chattering phenomenon in the responses and suppresses the chaotic oscillations in comparison with ordinary sliding mode control system. Responses of the feedback system depict the far-better performance of the proposed optimal sliding mode control from the viewpoint of reducing the settling time, overshoot, energy, and amortization in the suspension system.

Keywords Chaos · Power spectrum density · Optimal sliding mode control · Control Lyapunov function · Semi-active suspension

List of symbols

$x(t), \theta(t)$	Vertical displacement and pitch angular motion of sprung mass
$x_1(t), x_2(t)$	Heave motion of the unsprung masses
m, I	Mass and inertia moment of chassis
m_1, m_2	Masses of front and rear unsprung
l_1, l_2	Length of front and rear axels
x_{rp1}, x_{rp2}	Applied excitation displacement from the road surface on the front and rear tires,
K_{t1}, K_{t2}	Front and rear tire stiffness
C_{t1}, C_{t2}	Front and rear tire damping coefficient
$f_s, \Delta s$	Dynamic force and change of length of springs
k_s	Stiffness of the springs
f_d	Dissipative force in the MR fluid damper
C_d, C_0	Viscous damping at low and high velocity,
x_0	Piston relative displacement
α	Scaling value for the Bouc–Wen hysteresis loop

✉ S. Mahdi Abtahi
   m.abtahi@qiau.ac.ir; m_abtahi@dena.kntu.ac.ir

1 Faculty of Industrial and Mechanical Engineering, Qazvin Branch, Islamic Azad University, Nokhbegan Blvd., Qazvin, Iran

1 Introduction

Some of the vertical vibrations in the vehicle's chassis refer to the chaotic oscillations which cannot be damped using the passive suspension system. In the vertical motion of the vehicles, chaos phenomenon can be appeared due to the road surface unevenness and other properties of the nonlinear model. In addition to the passengers comfort subject in the vehicles, the chaotic vibrations can be caused the fatigue failure in the components of chassis and suspension system. Consequently, the researchers are motivated recently to analyze and control the vertical oscillations based on chaos [1–5]. In the vibrational analysis of bounce motion, first problem is the distinction of chaotic vibrations from the stochastic oscillations. For this purpose, chaotic behaviors can be proved using the mathematical and numerical methods for instance power spectrum density, Lyapunov exponent, and Poincare' sections [6–9].

Another main problem in the vertical displacement of vehicle is the control of chaotic vibrations using the

suspension system. Chaos control can be carried out via the nonlinear control algorithm based on the controllable suspension system. Therefore, the semi-active suspension on the basis of the magnetorheological (MR) fluid damper can be used to adjust the damping coefficient in the damper because of its simple structure and fast operation. The semi-active suspension utilizes a smart fluid with controllable viscosity in the MR fluid damper. The applied appropriate electrical current on the damper is produced using the controller system. Consequently, proper dissipative force in the damper is established in the suspension system in order to damp the bounce vibrations [10–12].

Due to highly nonlinear behavior in the MR fluid damper, a nonlinear control strategy must be designed for elimination of unwanted vibrations in the chassis of automobile. Sliding mode control algorithm is an appropriate robust controller especially for uncertain system. The parametric uncertainties in the system include the viscosity changes of oil with respect to temperature changes in damper, and changes in the mass of vehicle. The feedback semi-active suspension can be stabilized quickly using the SMC system. However, due to the switching function in SMC structure, the chattering phenomenon is occurred in the control system. In order to best eliminate the chattering, the optimal strategy can be combined with the SMC structure [13–16].

In the optimal sliding mode control (OSMC) scheme, the control signals are designed optimally according to the cost function in the control algorithm. In order to solve the optimal problem in the OSMC, the control Lyapunov function (CLF) method is used to find the optimal inputs and control gains. Thus, the CLF solves the Hamilton–Jacobi–Bellman equation with respect to the performance index via the Sontag's formula. Consequently in the OSMC, beside the quick stabilization due to the variable structure controller based on SMC, the chattering phenomenon can be rejected successfully because of the optimal system [15–21].

In the first section of this paper, the dynamical formulation of half-car model is derived based on the Newton–Euler equations. In the suspension system, in order to adjust the damping coefficient for control purposes, the semi-active suspension system is used based on the MR fluid damper. After simulation of the open-loop system under the fixed values of parameters in the MR fluid damper, chaos phenomenon is illustrated in the vertical motion of vehicles. In the next section, the power spectrum density (PSD) is used to study chaos in the system. Beside the PSD method, positive values of the largest Lyapunov exponents verify the results of PSD in the vibrating system. Moreover, trajectories of phase plane along with the Poincare' section of the open-loop system satisfy chaos. In the final section, for chaos control in the suspension system, the OSMC strategy is used to adjust the applied electrical current to the MR fluid damper for exact regulation of the viscosity and damping coefficient in the semi-active suspension. The results of the closed-loop system stress the superior performance of the optimal SMC system.

2 Dynamical model

In order to derive the mathematical model of the system, the equations of motion for the various parts of the system are calculated based on the half-vehicle model. The half-vehicle model of the system includes the chassis mass, front and rear axle mass, tires along with the elastic and dissipative effects according to Fig. 1.

The suspension system is also modeled with a semi-active type including the main springs and controllable dissipater that named MR fluid damper. In the semi-active suspension, the dynamical model of MR fluid damper with adjustable viscosity is derived on the basis of the modified Bouc–Wen model. The vertical displacement of the system is described using the second Newton's law, and the angular dynamics of the chassis is stated via the Euler equation as follows [1–3].

$$
\begin{aligned}
&m\ddot{x} + K_1 \mathrm{sgn}\left(x - x_1 - l_1 \sin\theta\right)\left|x - x_1 - l_1\sin\theta\right|^{n_1} + C_1\left(\dot{y}_1 - \dot{x}_1\right) + K_2\mathrm{sgn}\left(x - x_2 + l_2\sin\theta\right)\left|x - x_2 + l_2\sin\theta\right|^{n_2} \\
&\quad + C_2\left(\dot{y}_2 - \dot{x}_2\right) = 0
\end{aligned}
\tag{1}
$$

$$
\begin{aligned}
&m_1\ddot{x}_1 - K_1\mathrm{sgn}\left(x - x_1 - l_1\sin\theta\right)\left|x - x_1 - l_1\sin\theta\right|^{n_1} - C_1\left(\dot{y}_1 - \dot{x}_1\right) + K_{t1}\mathrm{sgn}\left(x_1 - x_{\mathrm{rp1}}\right)\left|x_1 - x_{\mathrm{rp1}}\right|^{n_{r1}} \\
&\quad + C_{t1}\left(\dot{x}_1 - \dot{x}_{\mathrm{rp1}}\right) = 0
\end{aligned}
\tag{2}
$$

$$
\begin{aligned}
&m_2\ddot{x}_2 - K_2\mathrm{sgn}\left(x - x_2 + l_2\sin\theta\right)\left|x - x_2 + l_2\sin\theta\right|^{n_2} - C_2\left(\dot{y}_2 - \dot{x}_2\right) + K_{t2}\mathrm{sgn}\left(x_2 - x_{\mathrm{rp2}}\right)\left|x_2 - x_{\mathrm{rp2}}\right|^{n_2} \\
&\quad + C_{t2}\left(\dot{x}_2 - \dot{x}_{rp2}\right) = 0
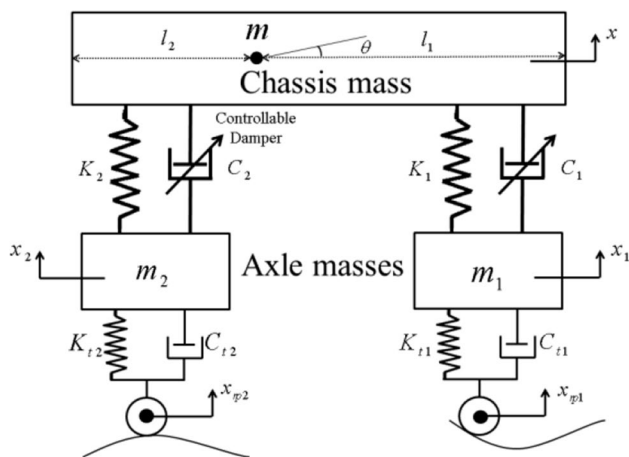\end{aligned}
\tag{3}
$$

Fig. 1 Vertical model of the vehicle system along with the semi-active suspension
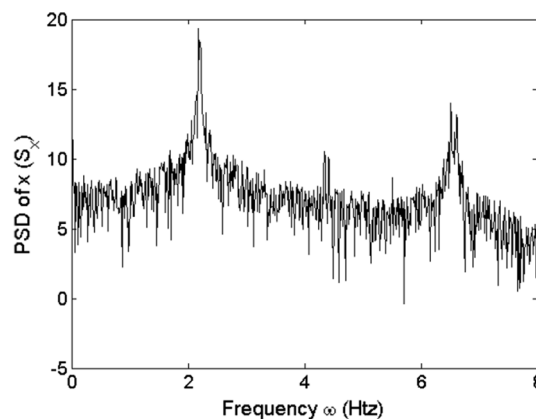

Fig. 2 Power spectrum density of the vertical displacement of the chassis

$$I\ddot{\theta} - \left[K_1 \mathrm{sgn}(x - x_1 - l_1 \sin\theta) |x - x_1 - l_1 \sin\theta|^{n_1} + C_1(\dot{y}_1 - \dot{x}_1) \right] l_1 \cos\theta$$
$$+ \left[K_2 \mathrm{sgn}(x - x_2 + l_2 \sin\theta) |x - x_2 + l_2 \sin\theta|^{n_2} + C_2(\dot{y}_2 - \dot{x}_2) \right] l_2 \cos\theta = 0, \tag{4}$$

where

$$\mathrm{sgn}(x) = \begin{cases} +1, & x > 0 \\ 0, & x = 0 \\ -1, & x < 0 \end{cases} \tag{5}$$

and "$n_{(1,2)}$" represents the nonlinearity order of the springs, and "$\dot{y}_{(1,2)}$" is the internal velocity in the MR fluid damper computing as:

$$\dot{y}_{(1,2)} = \frac{1}{(C_{0(1,2)} + C_{d(1,2)})} \left[\alpha Z + C_{0(1,2)}(\dot{x}_0 - l_{(1,2)}\dot{\theta}\cos\theta) \right] \tag{6}$$

In the above formula, indexes of (1, 2) are referred to the front and rear suspensions, respectively. Damping force in the MR fluid damper can also be calculated as follows:

$$f_d = C_{1,2} \left[\dot{y}_{(1,2)} - \dot{x}_{0(1,2)} \right] \tag{7}$$

Also, "Z" is the Bouc–Wen variable and is defined as follows.

$$\dot{Z} = -\gamma |(\dot{x} - l_1 \dot{\theta}\cos\theta) - \dot{y}_1| Z|Z|^{p-1} - \beta \left[(\dot{x} - l_1 \dot{\theta}\cos\theta) - \dot{y}_1 \right] |Z|^p + \delta \left[(\dot{x} - l_1 \dot{\theta}\cos\theta) - \dot{y}_1 \right], \tag{8}$$

where β, δ, γ and "p" are the fixed parameters in order to regulate the properties of the hysteresis loop in the MR fluid damper with respect to the magnetic field. Also C_0 and "α" are expressed as $\alpha = \alpha_a + \alpha_b I$ and $C_0 = C_{0a} + C_{0b}I$ as a functions of the applied electrical current to adjust the magnetic field in MR fluid damper. In the model of semi-active suspension system, the elastic force in springs is modeled as $f_s = k_s \mathrm{sgn}(\Delta_s)|\Delta_s|^n$ based on the nonlinear spring with fixed stiffness [11, 12].

In tire model, the spring action is also calculated similar to the main springs of the suspensions and dissipative effect is computed as $f_{dt} = C \dot{x}_{(1,2)}$ with constant damping coefficient. The profile of road unevenness is assumed as sinusoid function with frequency "f", amplitude of "A", and phase difference of "φ" in order to model the time delay between the excitation of the front and rear tires.

2.1 Chaos analysis in the open-loop system

The mathematical model of the vehicle system is simulated numerically using the Runge–Kutta method on the basis of the equations of motion. In order to simulate the uncontrolled system, a constant value for damping coefficient of the MR fluid damper is considered and the behavior of the open-loop system is analyzed under the initial conditions and constant parameters. Then, the chaotic vibrations are studied using the power spectrum density, Lyapunov exponent, Poincare' section, and phase portraits.

Power spectral density (PSD) is a numerical method in order to analyze the frequency response in a quasi-periodic or chaotic system. In this procedure, the signals are considered as independent of time using the Fourier transform of a time
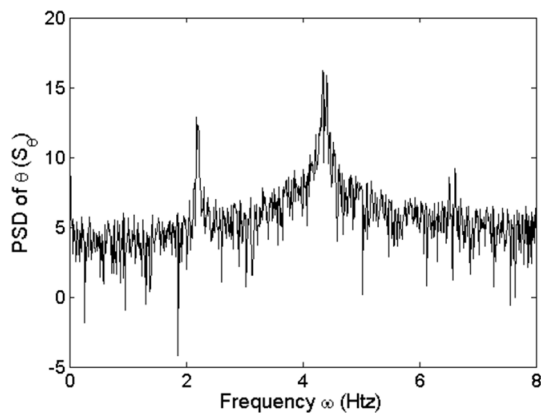
Fig. 3 Power spectrum density of the pitch angular motion of the chassis
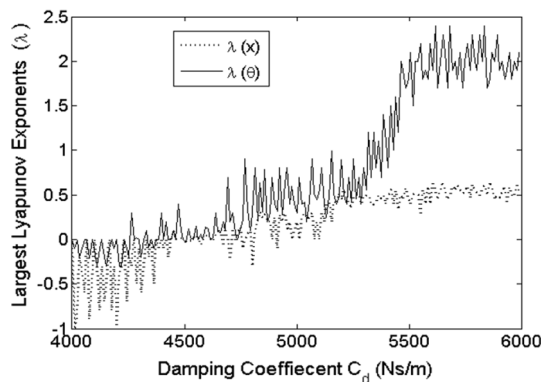

Fig. 4 Largest Lyapunov exponent with respect to the damping coefficient of MR fluid damper

series responses. The PSD is determined as the average of the Fourier transform magnitude squared, over a large time interval. Therefore, the PSD of a time series signal of variable $x(t)$ can be calculated as follows.

$$S_x(f) = \lim_{T \to \infty} \left\{ \frac{1}{2T} \left| \int_{-T}^{T} x(t)\, e^{-j2\pi ft} dt \right|^2 \right\} \qquad (9)$$

In the chaotic system, graph of PSD versus the frequency involves the wide range spectrum of the frequencies, while in the quasi-periodic systems the numbers of frequencies are limited. On the other words, in the chaotic system as Figs. 2 and 3, the PSD graph is demonstrated as spread spectrum along with disturbance [7, 9].

Moreover, the properties of the nonlinear system and chaos can be indicated via the Lyapunov exponent using the measurement of the gap between the two neighborhood orbits in the phase portrait. The Lyapunov exponent of $x(t)$ is calculated as follows.

$$\lambda = \lim_{t \to \infty} \frac{1}{t} \int_0^t E_i(x(\tau))d\tau = \lim_{t \to \infty} \frac{1}{t} \ln \left| \frac{\delta x(t)}{\delta x(0)} \right|, \qquad (10)$$

where $E_i(x(t))$ is the real part of the eigenvalue in the matrix that defines the rate of divergence in the system trajectories. The Lyapunov exponent of the vertical $x(t)$ and pitch $\theta(t)$ motion of the chassis are computed using the Wolf algorithm with respect to the damping coefficient of MR fluid damper as the control parameter. According to Fig. 4, when the damping coefficient is increased, the values of Lyapunov exponent become positive. It means the stretching, folding, and compressing of the trajectories show the occurrence of chaos in the system. On the other hand, the dynamical system can depict the hyper chaotic behavior, because the two variables of the system have the positive largest Lyapunov exponent [5–9].

Chaos analysis using the power spectral density and Lyapunov exponent can be validated via the simulation results based on the phase trajectories and the Poincare' section of the system as Fig. 5. According to Fig. 5, the basin of attraction in the open-loop system is a strange attractor based on the Fradkov definition due to the compressing, folding, and stretching orbits in the trajectories of the phase portraits. It means the phase portrait trajectories get away from the fixed point and again return to the neighborhood of equilibrium point that obviously reveals the compressing and stretching of the trajectories along with its folding. In fact, the strange attractor is an essential property in the chaotic system. Also, the chaotic responses can be illustrated due to the treatment of attractor as globally bounded and unstable locally on the basis of the Lyapunov stability criterion. Furthermore, according to the Devaney definition, chaos can be proved using the dense demonstration of points in the Poincare' section [8]. Therefore, chaos in the nonlinear system can be initially demonstrated using the phase space trajectories and Poincare' section. Then, chaos in the nonlinear system can be proved using the Lyapunov exponent. Finally, the results of Lyapunov exponents can be validated via the power spectrum density method for the chaotic vibrations.

2.2 Optimal sliding mode control strategy

The optimal sliding mode control is developed for a class of nonlinear systems as follows:

$$\begin{cases} \dot{x}_i = x_{i+1}, & i = 1, 2, \ldots, n-1 \\ \dot{x}_n = f(x) + u + \zeta \end{cases}, \qquad (11)$$

where $x = [x_1, \ldots, x_n]^T$ is the state vector, f is a smooth function, and ζ is a bounded disturbances. In this control scheme, a performance index as follows is to be minimized.

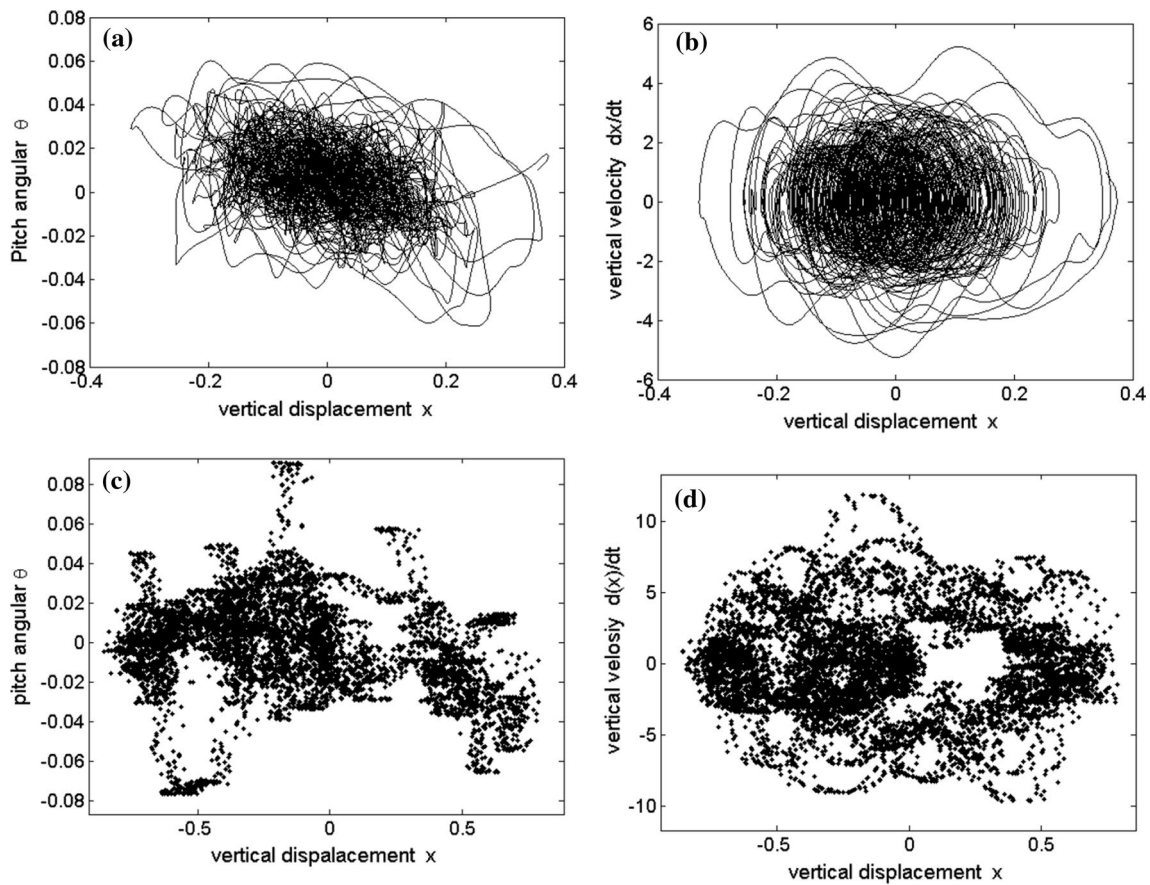$$I = \int_0^\infty (L(x) + u^2)dt, \qquad (12)$$

Fig. 5 Trajectories of phase portrait and Poincare' section in the open-loop system, **a** phase plane trajectory of $x - \theta$, **b** phase plane trajectory of $x - \mathrm{d}x/\mathrm{d}t$, **c** Poincare' section of $x - \theta$, **d** Poincare' section of $x - \mathrm{d}x/\mathrm{d}t$

that $L(x) \geq 0$ is a semi-definite positive function of the state x. For the purpose of the design of the robust control system around the fixed point, an integral SMC can be applied in the system with uncertainties [12–14]. In order to obtain optimality as well as robustness in this control strategy, the switching function is defined as:

$$s = c_1 x_1 + c_2 x_2 + \cdots + c_{n-1} x_{n-1} + x_n + \phi, \tag{13}$$

where $c_i's$ are constant parameters. Then, the approximated control input in SMC is designed continuously as follows.

$$u = -c_1 x_2 - c_2 x_3 - \cdots - c_{n-1} x_n - f - \dot{\phi} - M\sigma_\varepsilon(s) \tag{14}$$

where $M > \sup(\zeta)$, $\varepsilon > 0$ is a small constant, $\sigma_\varepsilon(.)$ is saturation function, ϕ is a smooth function that will be defined based on the Lyapunov stability via the positive definite Lyapunov function candidate as $V = s^{\mathrm{T}} s / 2$ where its derivative is semi-negative definite as:

$$\dot{V} = S\dot{S} = s\left(\zeta - \frac{M}{\varepsilon}s\right) = \varepsilon(|\zeta| - M) < 0, \tag{15}$$

that on the boundary of Ω, $s = |\zeta|$, and it establishes an invariant set in the feedback system. Since S always stays inside the Ω, the control input becomes,

$$u = -c_1 x_2 - c_2 x_3 - \cdots - c_{n-1} x_n - f - \dot{\phi} - \frac{M}{\varepsilon}s \tag{16}$$

Consequently, the dynamics of the closed-loop system is derived as:

$$\begin{cases} \dot{x}_i = x_{i+1}, \quad i = 1, 2, \ldots, n-1 \\ \dot{x}_n = -\eta c_1 x_1 - \sum_{i=1}^{n-1} (c_i + \eta c_{i+1}) x_{i+1} - \eta x_{n+1} - v, \\ \dot{x}_{n+1} = v \end{cases} \tag{17}$$

where $x_{n+1} = \phi$, $v = \dot{\phi}$, and $\eta = M/\varepsilon$. Then, the matrix form of the equations of motions in the feedback system is:

$$\dot{\bar{x}} = A\bar{x} + Bv \tag{18}$$

In this manner, the performance index becomes:

$$I = \int_0^\infty (L + \bar{f}^2 + 2\bar{f}v + v^2)\mathrm{d}t, \tag{19}$$

where A and B are the stabilizable matrices and,

$$\bar{f} = f + \eta c_1 x_1 + \sum_{i=1}^{n-1} (c_i + \eta c_{i+1}) x_{i+1} + \eta x_{n+1} \tag{20}$$

Using the OSMC, the equivalent problem is changed to an optimal control problem for a linear system with a non-quadratic cost function. To ensure the existence and uniqueness of the optimal control problem, the c_i's must be chosen until $L + \bar{f}^2 \succ 0$. In order to solve the optimal control problem for finding the optimal v, the control Lyapunov function approach is used [13–19].

3 Simulation of feedback system

In the closed-loop control system, solution of the optimal SMC problem based on the control Lyapunov function (CLF) method is summarized as follows.

$$\begin{cases} \underset{u}{\text{Min}} \quad \int_0^\infty (L(x) + u^2) dt \\ \text{subjected to :} \quad \dot{x}_n = F(x) + G(x)u \end{cases} \tag{21}$$

In the above optimal problem, the constraint is described as differential equations based on the dynamical model of the suspension system according to Eqs. (1–8). In order to solve the optimal control, firstly, $V(x)$ is selected as a candidate Lyapunov function. If $V(x)$ is a CLF, then it can solve the Hamilton–Jacobi–Bellman equation. Therefore, a suboptimal control input for the system with respect to the cost function in Eq. (12) can be given by Sontag's formula as following [17].

$$u^* = \begin{cases} -\dfrac{V_x F + \sqrt{(V_x F)^2 + L(V_x G)^2}}{V_x G} & ; V_x G \neq 0 \\ 0 & ; V_x G = 0 \end{cases}, \tag{22}$$

where $V_x = \partial V / \partial x$. In fact, in order to use the Sontag' formula, we need to find a CLF for the original system. On the other hand, using the optimal SMC, the nonlinear system can be transformed to a linear system as Eq. (18). Therefore, the appropriate values for c_i's must be selected that all the eigenvalues of matrix A are non-positive and different or have only one zero eigenvalue. In this manner, the switching function is derived in the new coordinate as:

$$s = c_1 x_1 + c_2 x_2 + \cdots + c_n x_n + x_n + x_{n+1} = C\bar{x} = \begin{bmatrix} c_1 & \dots & c_{n-1} & 1 & 1 \end{bmatrix} \bar{x} \tag{23}$$

According to the following Lemma and theorem, the appropriate CLF can be calculated to solve the optimal control problem [17].

Lemma 1 *Matrix A has all distinct eigenvalues in the left half of the plane with at most one at the origin; there exists a constant vector $H \in \mathbb{R}^{1 \times (n+1)}$ such that the Lyapunov equation $PA + A^{\mathrm{T}}P = -H^{\mathrm{T}}H$ has a positive semi-definite and symmetric solution P.*

Theorem 1 *If $\{B^{\mathrm{T}}P, H, C\}$ are linearly independent vectors in $\mathbb{R}^{1 \times (n+1)}$ and $P + C^{\mathrm{T}}C/2 \succ 0$, then function $V = \bar{x}^T P \bar{x} + s^2/2$ is a CLF for the system where P is the symmetric and positive semi-definite solution to the Lyapunov equation $PA + A^T P = -H^T H$ [17].*

Remark *If $P \succ 0$, then $P + C^{\mathrm{T}}C/2 \succ 0$ is satisfied for any C [18].*

According to Lemma 1, the solution of P in the Lyapunov equation is calculated as follows:

$$P = \int_0^\infty e^{tA^T} H^T H e^{tA} dt \tag{24}$$

The equations of motion based on the relations (1–8) are expressed again as state-space equation with definition of the following state variables as:

$$\bar{x}^{\mathrm{T}} = \begin{bmatrix} x_1 & \dots & x_8 \end{bmatrix}^{\mathrm{T}} = \begin{bmatrix} x & \dot{x} & x_1 & \dot{x}_1 & x_2 & \dot{x}_2 & \theta & \dot{\theta} \end{bmatrix}^{\mathrm{T}} \tag{25}$$

After simplification, in the closed-loop dynamical system based on the optimal SMC as Eq. (18), the linear matrices A and B are derived as:

$$A = \begin{bmatrix} 0 & 1 & 0 & \dots & 0 \\ 0 & 0 & 1 & \dots & 0 \\ \vdots & \vdots & \vdots & \dots & \vdots \\ -\eta c_1 & -(c_1 + \eta c_2) & \dots & \dots & -\eta \\ 0 & 0 & \dots & \dots & 0 \end{bmatrix}_{9 \times 9}, \quad B = \begin{bmatrix} 0 \\ \vdots \\ 0 \\ -1 \\ 1 \end{bmatrix}_{9 \times 1} \tag{26}$$

Whereas the matrix H is fixed, H is assumed as $H = \begin{bmatrix} 1 & \dots & 1 \end{bmatrix}_{1 \times 9}$. In order to calculate P based on Eq. (24), we have

$$e^{tA} = T \begin{bmatrix} e^{\lambda_1 t} & 0 & \dots & 0 \\ 0 & \ddots & & \vdots \\ \vdots & & \ddots & 0 \\ 0 & \dots & 0 & e^{\lambda_9 t} \end{bmatrix} T^{-1}, \tag{27}$$

that λ_1 to λ_9 are the eigenvalues of the A and T is a matrix that its columns are the eigenvectors of A. After calculating P, the CLF is derived as equation $V = \bar{x}^{\mathrm{T}} P \bar{x} + s^2/2$. Consequently, with substituting the $V(x)$ as a CLF into the Sontag' formula, we can obtain a suboptimal SMC structure. In order to apply the Sontag's formula, the cost function is modified

by neglecting the cross term between the state and the control input as:

$$I = \int_0^\infty (L + \bar{f}^2 + v^2)\mathrm{d}t = \int_0^\infty (\bar{L} + v^2)\mathrm{d}t, \tag{28}$$

where $\bar{L} = L + \bar{f}^2$. Then, the switching function in this algorithm is become:

$$s = \sum_{i=1}^{n-1} c_i x_i + x_n + \phi \tag{29}$$

Finally, the control input is computed as follows.

$$u = -\sum_{i=1}^{n-1} c_i x_{i+1} - f - \dot{\phi} - \eta s, \tag{30}$$

which in that,

$$\dot{\phi} = \begin{cases} -\dfrac{V_x A \bar{x} + \sqrt{(V_x A \bar{x})^2 + L(V_x B)^2}}{V_x B}; & V_x B \neq 0 \\ 0; & V_x B = 0 \end{cases}, \tag{31}$$
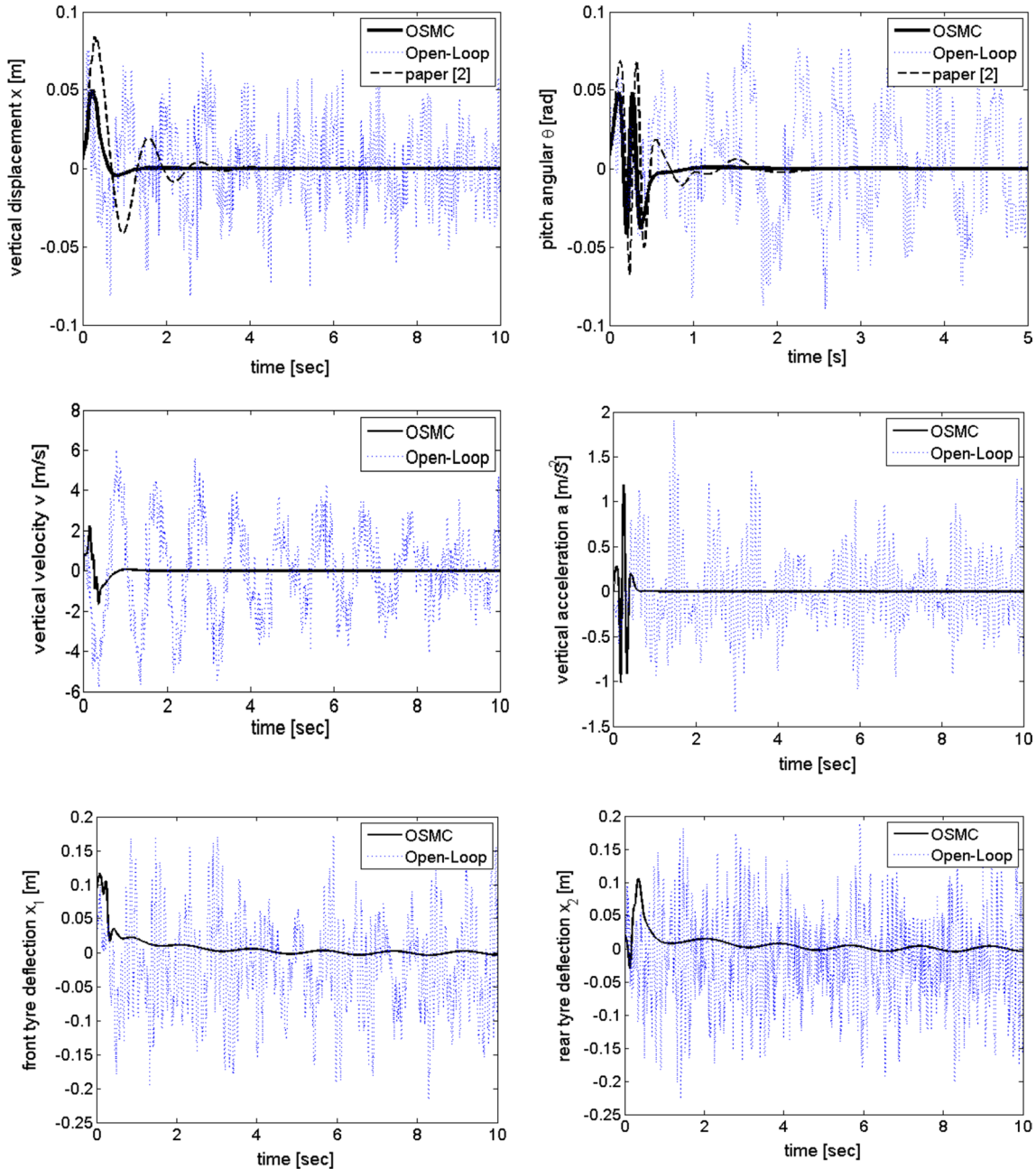

Fig. 6 Closed-loop responses of the system based on the OSMC against the chaotic open-loop behavior
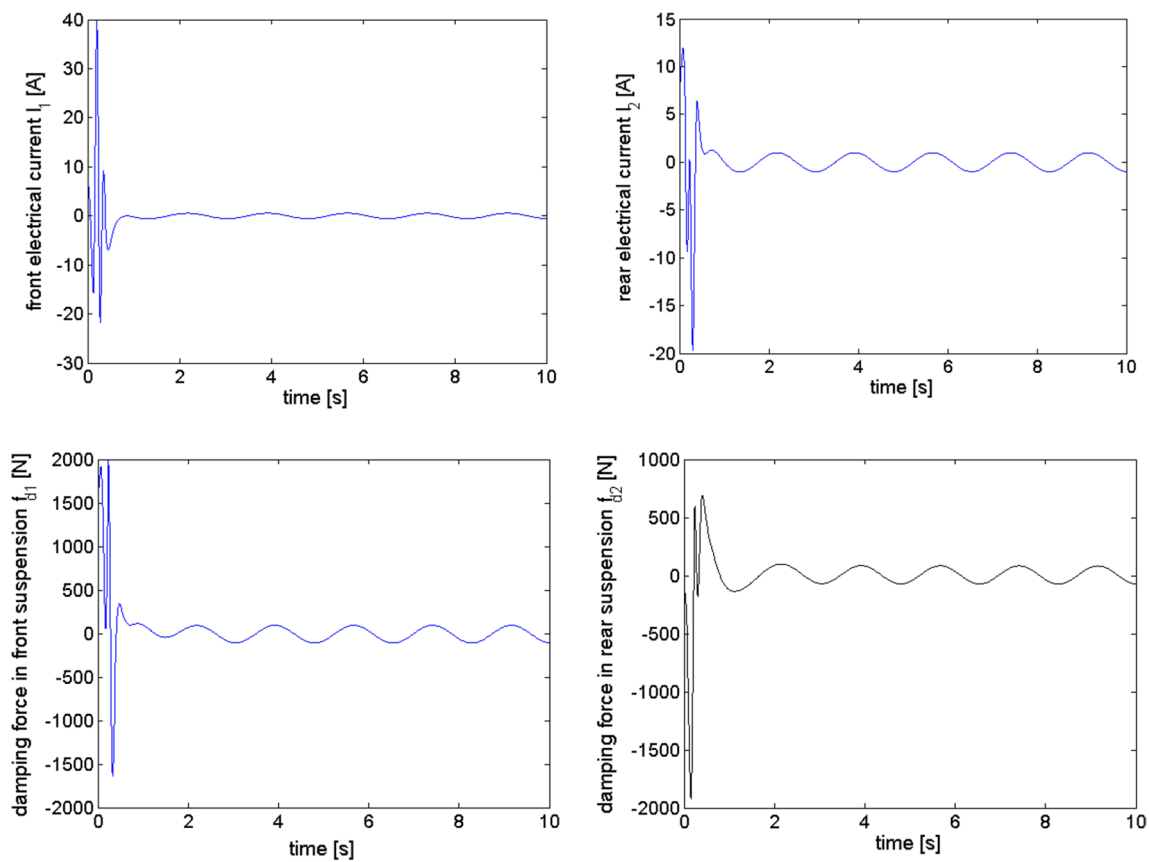
Fig. 7 Applied electrical current and damping force in the MR fluid damper under the OSMC system

Table 1 The values of the control gains in the OSMC algorithm

c_1	c_2	c_3	c_4	c_5	c_6	c_7	c_8
3.85	2.04	0.03	0.17	1.02	0.28	5.12	1.70

Table 2 The values of the parameters of the system

m (kg)	I (kgm^2)	m_1 (kg)	m_2 (kg)	K_1 (N/m)	K_2 (N/m)	C_{t1} (Ns/m)	C_{t2} (Ns/m)	K_{t1} (N/m)	K_{t2} (N/m)	l_1 (m)	l_2 (m)
1800	2200	60	60	35,000	36,000	10	10	190,000	190,000	1.7	1.4

and

$$\phi(0) = -\sum_{i=1}^{n-1} c_i x_i(0) - x_n(0) \tag{32}$$

On the basis of the above-mentioned calculations, simulation of the feedback system based on the OSMC is shown in Figs. 6 and 7 under the values of the control gains c_i's as following in Table 1. All of the simulations were carried out on the basis of the numerical solution of above equations using the fourth-order Runge–Kutta method. Also, the values of parameters in the simulation system are stated in Table 2.

Responses of the feedback system based on the optimal sliding mode control are demonstrated in Fig. 6. According to these figures, stabilization of the suspension system is depicted at a few time and overshoot along with chaos suppression. Vertical displacement of chassis, velocity, and acceleration of car body and angular pitch motion of vehicle is reached to the desired value in less than about 1.5 s. Whereas the behavior of the system under SMC includes the chattering phenomenon, the chattering can be eliminated using the combination of optimal control with the SMC structure. Therefore, the major point in the closed-loop responses is the rejection of chattering phenomenon. Also, behavior of the tires deflection can be

acceptable against the motion of tires on the sinusoidal profile road.

Also, the results of feedback system under the optimal sliding mode control in this work are compared with the results of paper [2] especially, because the chaotic model of vehicle along with the parameters values in this work and paper [2] is totally similar. Also, chaos control algorithm in paper [2] is on the basis of the optimal OGY method. According to Fig. 6, comparison of simulation results depicts that the feedback system under the optimal sliding mode control reduces impressively the settling time and over shoot relative to chaos controller in [2] due to the rapid stabilization to the fixed point in the sliding mode control algorithm via the sliding surface properties in variable structure control scheme.

Performance of the actuators in feedback system is also illustrated in Fig. 7. In the semi-active suspensions system, applied forces of the MR fluid damper play the role of control input. Actually, the vibrations resulting the unevenness road surface can be damped using the dissipative force in the magnetic dampers. In the MR fluid damper, the damping forces can be adjusted using the applied electrical current to the dampers.

4 Conclusions

In this paper, chaos control in the semi-active suspension system is considered on the basis of the chattering-free optimal sliding mode control. For this purpose, the mathematical model of the system is first derived using the Newton–Euler equations. According to the simulation results of the uncontrolled system, the chaotic oscillations are appeared in the vertical motion of the suspension system. In order to chaos study, the power spectrum density and Lyapunov exponents evaluate chaos numerically. The results of the chaotic analysis based on the PSD and LE depict the occurrence of chaos. Also, the phase portrait trajectories and the Poincare' section confirm chaos in the system. In order to suppress the chaotic vibrations in the system, a feedback controller based on the optimal SMC is applied for the semi-active suspension system. Beside the appropriate stabilization of the chaotic vibrations, the major point of the OSMC algorithm is the rejection of chattering in comparison with SMC. The simulation results of OSMC system demonstrate the reduction of 31% in the energy consumption relative to [11] and the reduction of 14% in comparison with [2]. Moreover, the responses of the feedback system depicts the reduction of 22% in settling time toward [11] and the reduction of 8% relative to [2].

References

1. Litak G, Borowiec M, Friswell MI, Szabelski K (2008) Chaotic vibration of a quarter-car model excited by the road surface profile. Commun Nonlinear Sci Numer Simul 13:1373–1383
2. Abtahi SM (2017) Chaotic study and chaos control in a half-vehicle model with semi-active suspension using discrete optimal Ott–Grebogi–Yorke method. Proc IMechE Part K J Multi-body Dyn IMechE 231:148–155
3. Yang Z, Zhou Y; Liang S (2017) Sliding mode control of chaos vibrations in 7-DOF nonlinear active vehicle suspension. In: Proceedings of the 2017 international conference on advanced mechatronic systems, Xiamen, China, 6–9 December 2017
4. Zhu Q, Ishitobi M (2006) Chaotic vibration of a nonlinear full-vehicle model. Int J Solids Struct 43:747–759
5. Yang Z, Liang S, Sun Y, Zhu Q (2014) Vibration suppression of four degree-of-freedom nonlinear vehicle suspension model excited by the consecutive speed humps. J Vib Control 3:1–8
6. Abtahi SM, Sadati SH, Salarieh H (2016) Nonlinear analysis and attitude control of a gyrostat satellite with chaotic dynamics using discrete-time LQR-OGY. J Asian J Control 18:1845–1855
7. Sun Y, Xiong G, Ma X, Gong J, Chen H (2015) Quantitative evaluation of unmanned ground vehicle trajectory based on chaos theory. Adv Mech Eng 7:11–24
8. Abtahi SM, Sadati SH (2013) Chaos control in attitude dynamics of a gyrostat satellite based on linearised Poincare' map estimation by support vector machine. Proc IMechE Part K J Multi-body Dyn 227:302–312
9. Hilborn R (2000) Chaos and nonlinear dynamics: an introduction for scientists and engineers. Oxford University Press, New York
10. Wang Y-H, Shih M-C (2012) Effect of a hybrid controller on ride comfort under random road excitation for a semi-active suspension system. Proc Inst Mech Eng Part D J Automob Eng 226:1640–1651
11. Lozoya-Santos J, Morales-Menendez R, Ramirez-Mendoza RA, Sename O (2013) Adaptive semi-active suspension design using gain-scheduling. IFAC Proc Vol 46:845–850
12. Zong L, Gong X, Xuan S, Guo C (2013) Semi-active H_∞ control of high-speed railway vehicle suspension with magnetorheological dampers. Veh Syst Dyn 51:600–626
13. Doostdar P, Keighobadi J (2012) Design and implementation of SMO for a nonlinear MIMO AHRS. Mech Syst Signal Process 32:94–115
14. Yuvapriya T, Lakshmi P, Rajendiran S (2018) Vibration suppression in full car active suspension system using fractional order sliding mode controller. J Braz Soc Mech Sci Eng 40:217–227
15. Keighobadi J, Sadeghi MS, Fazeli A (2011) Dynamic sliding mode controller for trajectory tracking of nonholonomic mobile robots. Preprints of the 18th IFAC world congress, Milano, Italy, 28 August 2011
16. Keighobadi J, Hosseini-Pishrobat M (2017) Robust output regulation of a triaxial MEMS gyroscope via nonlinear active disturbance rejection, Int J Robust Nonlinear Control, https://onlinelibrary.wiley.com/doi/abs/10.1002/rnc.3983, Accessed 22 Nov 2017
17. Salamci MU, Kemal-Oslash M, Zg-ograve R, Stephen P (2000) Sliding mode control with optimal sliding surfaces for missile autopilot design. J Guid Control Dyn 23:719–727
18. Freeman RA, Kokotovic PV (1996) Inverse optimality in robust stabilization. SIAM J Control Optim 34:1365–1391
19. Pang H, Yang X (2013) Robust optimal sliding-mode tracking control for a class of uncertain nonlinear MIMO systems. J Appl Math 1:863168–863177
20. Keighobadi J, Yarmohammadi M (2016) New chatter-free sliding mode synchronization of steer-by-wire systems under chaotic conditions. J Mech Sci Technol 30:3829–3834

21. Oveisi A, Hosseini-Pishrobat M, Nestorović T, Keighobadi J (2018) Observer based repetitive model predictive control in active vibration suppression, J Int Assoc Struct Control Monit https://onlinelibrary.wiley.com/doi/abs/10.1002/stc.2149, Accessed 13 February 2018